Active polarization independent coupling to silicon photonics circuit

J. Niklas Caspers[a], Yun Wang[b], Lukas Chrostowski[b] and Mo Mojahedi[a]

[a]Department of Electrical and Computer Engineering, University of Toronto, 10 King's College Road, Toronto, ON, M5S 3G4, Canada;
[b]Department of Electrical and Computer Engineering, University of British Columbia 2332 Main Mall, Vancouver, BC, V6T 1Z4, Canada

ABSTRACT

We have experimentally demonstrated the ability to couple an arbitrary polarization state from a fiber to the TE-mode of a single waveguide in an integrated silicon photonics circuit with an extinction ratio larger than 31 dB, measured between the output ports of the integrated photonic circuit. To achieve this we combined a 2D-grating coupler and a Mach-Zehnder Interferometer (MZI). After accounting for setup and coupling losses, for a 1 mW input into the 2D coupler, we obtain an average output power of 0.98 mW at the desired waveguide, with less than 1.2 dB variation across all input polarization states. The experiments were performed at a wavelength of 1.55 μm.

Keywords: Silicon Photonics, Polarization Control, MZI, Grating Coupler, Integrated Optics

1. INTRODUCTION

Silicon photonics allow for larger bandwidth optical communication on chip, but needs to be interfaced with optical fibers to transport information on/off the chip.[1] The polarization in an optical fiber can change due to induced stress or temperature changes and light can be transfered between the two orthogonal polarization components. On the other hand silicon waveguides can be designed to have both polarizations present (TE & TM), but their mode properties such as effective index, mode confinement and others will be different for the two polarizations. Thus a silicon photonics device designed for one polarization will often not have the same performance or not work at all for the other polarizations.[2] This is especially the case for the high-confined waveguides where the SOI thickness is 220 nm, as commonly offered by multi-project wafer foundry services.

This means that in addition to the large mode-size mismatch[3] between the optical mode in integrated waveguides and the mode in an optical fiber, there is a polarization incompatibility, which needs to be addressed. If not addressed, the transmission and performance of the photonic circuit will be unstable. A straight-forward approach is to avoid the problem from occurring. In this case this would mean to either have the silicon waveguides polarization insensitive or the optical mode in the fiber to maintain its polarization.

An etched silicon waveguide could in theory be made polarization insensitive, by controlling its width and height accurately. A perfectly square waveguide would still have a TM & TE mode, but their effective indexes would be the same if the waveguide is straight. On the other hand, when the waveguide is bent in the plane, for example in a micro-ring resonator, where the goal is to have the same resonance frequencies, the cross-section would need to be slightly rectangular. In a ring resonator the height and width of the waveguide would need to be controlled with a subatomic precision to prevent a shift in resonance frequency by more then a fraction of the width of the resonance.[2] This is neither technologically nor economically feasible.

Alternatively, one could make fibers that a polarization maintaining. Polarization maintaining fibers have been a commercial product for some time now and thus would be an alternative. However, they tend to have larger dispersion, are more expensive, and would have to be specifically aligned when being connected to the photonics circuit.[4] Thus while currently used in most research labs, they should be avoided in a large scale integration.

J. Niklas Caspers: E-mail: n.caspers@utoronto.ca, Telephone: 1 647 380 0123, Web: www.mogroup.utoronto.ca

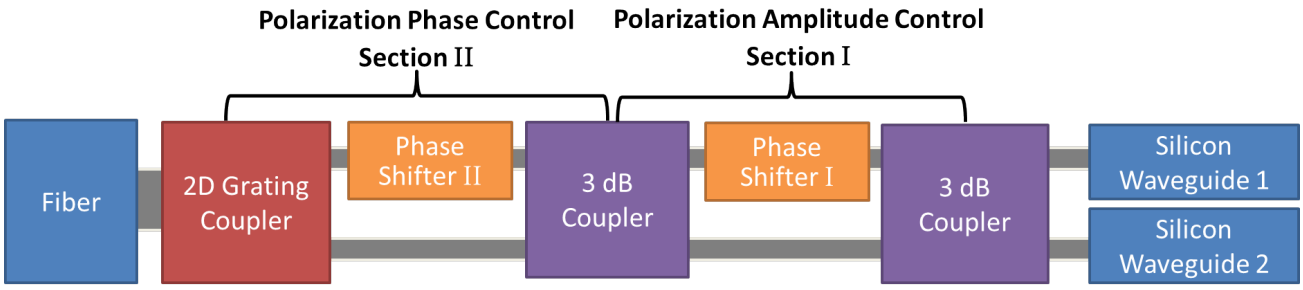

Figure 1. Diagram of the proposed tunable rotator with its functional elements.

In summary a solution has to be found to interface an optical fiber with a photonics circuit while removing the polarization incompatibility without putting restrictions on either the fibers or the photonics waveguides. A currently widely accepted solution is polarization diversity.[2] The light is coupled to the photonic circuit from the fiber and then split into the TE and TM component. Usually the TM component is rotated to the TE mode and the light is processed in two identical circuits. Recent demonstrations of different functionalities using polarization diversity include an optical clock.[5] Passive functionalities can be realized by utilizing the forward and backward propagating modes as previously demonstrated.[6] However utilizing the forward and backward component to remove the need of two circuits is limited to simple passive circuits. Any more complex functionality or even active circuits would require two optical circuits. Thus the power consumption and space requirement would be doubled for active polarization diversity circuits.

A more elegant solution would be to ensure that the random polarization from the fiber could be efficiently coupled to only the TE mode of a single waveguide. The light could then be modulated, wavelength (de-) multiplexed, or just measured in a single optical circuit. Such an approach would require an active compensation to cope with changes of the incoming polarization state due to temperature and strain fluctuations in the fiber. While this approach might require extra power and space compared to a purely passive approach, these requirement would be more then compensated by not requiring two optical circuits for light and information processing. Thus it would be advantageous for any larger active circuit, because only one optical circuit is needed instead of two in the polarization diversity approach.[7] An active polarization control could also be used for many more applications, such as: more advanced modulation schemes to encode information onto the polarization state, quantum key distribution systems, and sensing applications. Such active polarization control can also be used in reverse, coupling light off the chip, where it is possible to create an arbitrary output polarization state for sensing or other applications*. Lastly, the circuit can be used to measure the incoming polarization state, i.e. the stokes parameter of the incoming light. This idea of linear optical circuits has recently also been proposed by Miller.[9]

The system we propose and partially realized is shown as a block diagram in Fig. 1. A 3D schematic is shown in Fig. 2. The system can be used in both directions, but it is more intuitive to understand if the light is coming from the chip and is coupled into a fiber. Light in the TE mode of a silicon nanowire is split between two branches using a 3 dB coupler. One of the branches has a phase shifter to change the relative phase between the two arms. A second 3 dB coupler is used to couple the arms back together. The output of the second 3 dB is split again into two branches. The power splitting ratio between the second two branches is determined by the relative phase difference, controlled by the first phase shifter. One of the arms again has a phase shifter and both arms are used as the two inputs into a 2D grating coupler.[10,11] Thus the light output is coupled onto two orthogonal polarization states in the fiber, where the amplitude between the two polarizations is controlled by the first phase shifter, while the phase is controlled by the second phase shifter.

2. THEORETICAL PROOF OF OPERATION

In the following section the systems response will be described mathematically for both directions: light incident from a single silicon waveguide and collected using a fiber; as well as light coupled from a fiber into the circuit.

*After submission of this work the idea of active polarization control has also been published by Sacher et. al.[8]

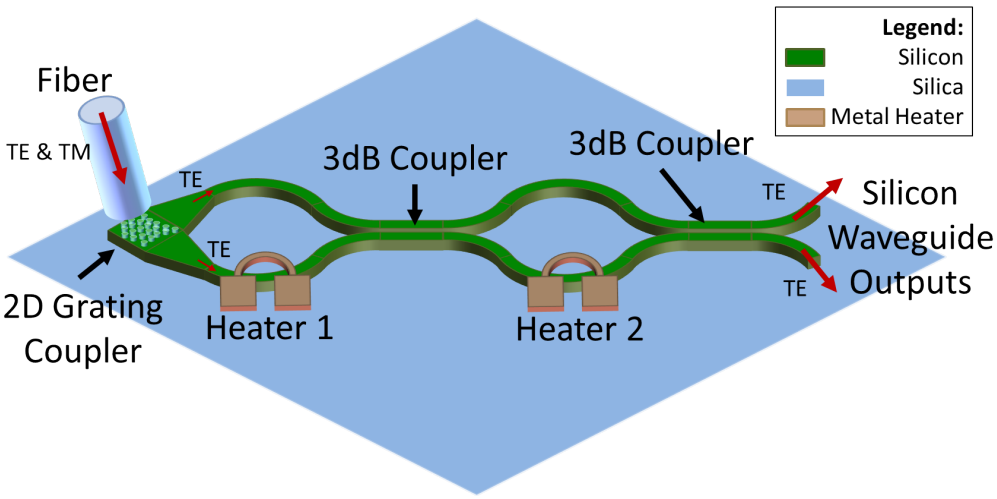

Figure 2. An artistic vision of the rotator system with all its elements.

We will prove that both an arbitrary polarization state can be coupled without additional loss from the fiber to the TE mode of a single silicon waveguide, as well as that an arbitrary polarization state can be injected into a fiber.

2.1 Input: Silicon Waveguide

The description of this approach is based on a transfer matrix approach, more information about this approach can for example be found in.[12] The top and bottom waveguides are treated as the two components of a 2D vector. The 3 dB coupler $\bar{T}$ and the propagation in the two arms with the phase shifter $\bar{P_m}$ can be described using the following two matrices:

$$\bar{T} = \frac{1}{\sqrt{2}} \begin{pmatrix} 1 & 1 \\ 1 & -1 \end{pmatrix} \tag{1}$$

$$\bar{P_m} = \begin{pmatrix} e^{i\phi_m} & 0 \\ 0 & e^{i\phi_{m'}} \end{pmatrix} = e^{i\phi_m} \begin{pmatrix} 1 & 0 \\ 0 & e^{i\Delta\phi_m} \end{pmatrix}; \tag{2}$$

Here, $\phi_m = L \cdot \beta$ is the phase accumulated due to the propagation in one of the arms with length L in the section m for light propagation with the propagation constant β. We defined $\Delta\phi_m = \phi_{m'} - \phi_m$ as the difference in phase between the two arms, which can be induced using a heater or by a difference in propagation lengths.

First we will describe the case when light is coming from waveguide 1, thus we will use the following normalized input vector:

$$\vec{a}_0 = \begin{pmatrix} 1 \\ 0 \end{pmatrix}. \tag{3}$$

The output of the complete system can then be calculated by multiplying the matrices from Eq. 1 and 2, also refer to Fig. 1:

$$\begin{aligned} \vec{a}_{end} &= \bar{P_{II}} \cdot \bar{T} \cdot \bar{P_I} \cdot \bar{T} \cdot \vec{a}_0 \\ &= \frac{e^{i(\phi_I + \phi_{II})}}{2} \begin{pmatrix} (1 + e^{i\Delta\phi_I}) \\ e^{i\Delta\phi_{II}}(1 - e^{i\Delta\phi_I}) \end{pmatrix}. \end{aligned} \tag{4}$$

The global phase $\phi_I + \phi_{II}$ can be neglected, while the relative phases between the two components controls the output state in the fiber. The two parts of the final vector $\vec{a}_{end}$ are the two orthogonal polarizations in the fiber. The grating coupler converts the two waveguide inputs with the same polarization into one output (fiber) but orthogonal polarization, generally referred to as s- and p-polarization. This separate waveguide to orthogonal polarization conversion can be considered a geometrical polarization rotation.[7]

The output vector $\vec{a}_{end}$ can be analyzed further. Of interest could *e.g* be the magnitude off the two output polarization, referred to here as s and p.

$$|E_s|^2 = \frac{1}{2}\sqrt{(1+e^{i\Delta\phi_I})(1+e^{-i\Delta\phi_I})}$$
$$= cos^2(\frac{1}{2}\Delta\phi_I) \quad (5)$$
$$|E_p| = sin^2(\frac{1}{2}\Delta\phi_I) \quad (6)$$

As expected the magnitude of the fields is controlled by the relative phase difference induced in section I. Thus by passing a current through Heater I, the relative phase can be changed and thus the relative power between the two polarizations at the output will change.

To switch between a linear polarization and a circular polarization one also needs to control the relative phase between the s- and p-polarization. It is clear from Eq. 4, that the governing component is $\Delta\phi_{II}$, which can be controlled using Heater 2. The phase shifter in Section 1 will also introduce a phase between the two output polarizations, but as long as Heater 2 can be tuned from 0 to 2π, this can be compensated for.

In summary we have derived that using the proposed system one can couple light from one waveguide into an arbitrary polarization state off the chip.

2.2 Input: Optical Fiber

All the components used in the system (couplers, waveguides, phase shifters, grating couplers) have a linear response and are Helmholtz reciprocal,[13] thus any linear combination of them will also be reciprocal.[13] By proving that the input of one waveguide can be mapped onto any output polarization state in the fiber, it is thus also proven that light in any polarization state coming from the fiber can be guided to a single waveguide.

However, a separate proof for light coming from the fiber to be coupled to a single waveguide provides additional insight. Thus it is provided in the following section.

An arbitrary input polarization state can be described with the following normalized vector,

$$\vec{a}_{Pol} = \begin{pmatrix} a_1 e^{i\phi_1} \\ a_2 e^{i\phi_2} \end{pmatrix} \equiv \begin{pmatrix} a \\ \sqrt{1-a^2}e^{i\phi_a} \end{pmatrix}; \quad \phi_a = \phi_2 - \phi_1 \quad (7)$$

where a, a_1, a_2 and ϕ_a, ϕ_1, ϕ_2 are real numbers and $0 \leq a \leq 1$. The global phase is again neglected. The elements of $\vec{a}_{Pol}$ are the complex field amplitudes of the vertical and horizontal polarization as described in e.g.[12]

The 2D grating coupler converts the two polarization states into the TE mode of two separate silicon waveguides. The state vector will not be changed by this however, $\vec{a}_{Pol} = \vec{a}_{Grat}$. We are assuming an ideal coupler with no differential phase shift. There will be also in general an insertion loss associated with the coupling, but well designed coupler can at least minimize any difference in coupling for the two polarization components[11]

A phase shifter followed by a 3 dB coupler is located after the grating coupler, which introduces a phase in one of the arms. This phase control will allow the light to be split 50:50 after the second 3 dB coupler, independent of the amplitude distribution before the coupler. This splitting is achieved by controlling the phase difference between the polarization by choosing the phase (ϕ_I) introduced by the first heater accordingly.

The state vector after the first 3 dB coupler can be calculated as follows

$$\vec{a}_{Coup1} = \bar{T} \cdot \bar{P_{II}} \cdot \vec{a}_{Grat} = \frac{1}{\sqrt{2}} \begin{pmatrix} a + \sqrt{1-a^2}e^{i(\phi_a+\phi_{II})} \\ a - \sqrt{1-a^2}e^{i(\phi_a+\phi_{II})} \end{pmatrix} \overset{\phi_a+\phi_{II} \equiv \frac{\pi}{2}}{=} \frac{1}{\sqrt{2}} \begin{pmatrix} a + i\sqrt{1-a^2} \\ a - i\sqrt{1-a^2} \end{pmatrix} = \frac{1}{\sqrt{2}} \begin{pmatrix} e^{i\Phi} \\ e^{-i\Phi} \end{pmatrix}. \quad (8)$$

As indicated the phase introduced by the second phase shifter (please refer to Fig. 1 for the numbering), ϕ_{II}, has to be chosen such that $\phi_a + \phi_{II} \equiv \pm\frac{\pi}{2}, \pm\frac{3\pi}{2}, \pm\frac{5\pi}{2}$. In the last equation the Cartesian representation of the amplitude is rewritten into polar form and the following identities are used,

$$\left| a + \pm i\sqrt{1-a^2} \right| = \sqrt{a^2 + (1-a^2)} = 1, \quad \forall a \quad (9)$$
$$\arg\left(a + \pm i\sqrt{1-a^2} \right) := \pm\Phi. \quad (10)$$

To stress this result again, independent of the input amplitude distribution the power distribution after the first 3 dB coupler will be 50:50, by only adjusting the phase. The second phase-shifter with the second 3 dB coupler will now be adjusted to ensure that all the power can be coupled into a single output waveguide.

$$\vec{a}_{Out} = \bar{T} \cdot \bar{P}_I \cdot \vec{a}_{Coup1} = \frac{e^{-i\Phi}}{2} \begin{pmatrix} e^{i(2\Phi+\phi_I} + 1 \\ 1 - e^{i(2\Phi+\phi_I} \end{pmatrix} \overset{2\Phi+\phi_I \equiv 0}{=} e^{-i\Phi} \begin{pmatrix} 1 \\ 0 \end{pmatrix} \tag{11}$$

By tuning the first phase shifter in such way that $2\Phi + \phi_I \equiv 0, \pm 2\pi, \pm 4\pi, ...$ the light will be fully coupled to one, in this case the top waveguide.

$$T_{out} = 1 \tag{12}$$

where T_{out} is the normalized transmitted power in the wanted waveguide. Thus importantly, there are no system inherent losses. The only losses are component losses which would arise for an polarization diversity approach as well.

A few limitations can however arise:

1. For describing the 3 dB coupler an ideal response was assumed, in reality the coupling coefficients are often not exactly $\frac{1}{\sqrt{2}}$. The use of an adiabatic coupler in our design helps to reduce this problem. Also, the phase was assumed to be equal, whereas a directional coupler has a $\pi/2$ phase difference at the output. This phase difference would not change the general results, but change the phases the shifters have to introduce to get the same result.

2. The two arms of the MZI might be unbalanced in both lengths and loss. A too large imbalance in lengths will reduce the bandwidths of the device, while an imbalance in loss in the second MZI will reduce the performance of the device.

3. The analysis was only performed for a single wavelength. If the polarization state is the same for all wavelengths, the bandwidth limitation will arise due to a non-flat response of the phase shifter. A heating based phase shifter will have a limited bandwidth, as the induced phase shift is ($\Delta\phi = \frac{2\pi}{\lambda} L \frac{dn_{eff}}{dT} \Delta T$) wavelength dependent. Thus the polarization transparent system will be spectrally limited. Additionally, the polarization state might not be the same for all wavelengths. One can assume though that it will be stable over at least roughly one of the telecommunication bands (∼50 nm).[7]

3. FABRICATION AND LINEAR TRANSMISSION RESULTS

As a first proof of principle experiment we designed a system that does not require fabricated heaters, but can be tuned by changing the sample temperature. However, as the temperature can only be tuned for the whole sample, only either the phase between the two polarizations or the power distribution can be changed. Thus this system will be able to couple all the light of a fiber into one waveguide but only for a subset of polarizations.

The GDS layout of the system is shown in Fig. 3. Red regions are protected areas during the first etch resulting in a layer of 220 nm silicon. Yellow areas are used for the second etch, which is a partial etch of 70 nm; this partial etch results in a silicon thickness of 150 nm where both the red and yellow are drawn. A fiber array with a 127 μm spacing between the fibers will be aligned to the three grating couplers at the bottom. Light can be sent into the 2D grating coupler on the very left and gets split into the orthogonal polarization components. The two outputs of the 2D grating coupler are connected to an adiabatic coupler, which mixes the light of the two arms. A second adiabatic coupler is located after the first, in the GDS underneath the first one. The waveguides between the two adiabatic couplers have different lengths, which causes a wavelength dependent phase shift between the two arms. The sample stage temperature is controlled and thus used to change the phase shift. The output of the system is accessed using two 1D grating couplers. The unbalanced MZI had an offset in length of 70 μm, where the offset is visible in the difference in waveguide lengths between the two adiabatic couplers in the top right.

The 2D grating couplers were designed by overlapping a number of focusing ellipses at an orthogonal angle and placing scattering centers at the intersections similar to.[10] The 1D grating couplers are based on a previous design[14] and the adiabatic couplers are a slight improvement of a previous design by Han Yun.[15]

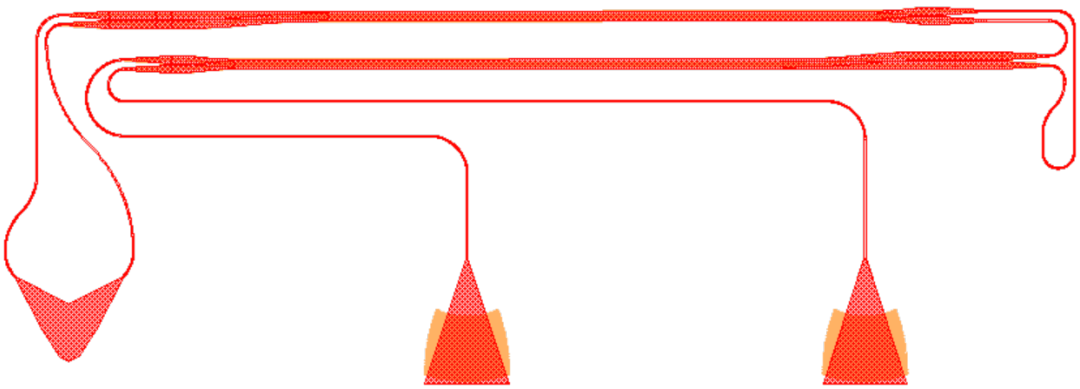

Figure 3. Screenshot of the gds layout of the fabricated proof of principle devices.

The samples were fabricated using e-beam lithography, which first wrote the full etch pattern into resist. The pattern was then transfered using reactive ion etching. The partial etch pattern was done similarly afterwards. The resulting structure with a top oxide cladding is shown in Fig. 4.

For the sample characterization light from an Agilent tuneable laser source is coupled into a polarization maintaining fiber (PMF) and coupled onto the chip using a fiber array. The fiber array consist of 8 PMF fibers in a line with a spacing of 127 μm, whereas one fiber is used as an input and connected to the laser, while the other fibers are connected to power meters to measure the transmitted power. This set spacing allows for a fast alignment between the fibers and grating couplers on chip and combined with an automated setup allows for linear transmission data of thousands of devices in mere hours.[16,17]

To first demonstrate the switching between output ports we measured the transmission spectrum of our system. The normalized transmission is shown in Fig. 5. The light was incident on the 2D grating coupler and had the electric field polarized horizontally. Due to the unbalanced MZI the light is switching between the two outputs as a function of wavelengths. The spectrum shown here can be tuned by changing the sample temperature. Additionally, while not shown here, other polarization states would show the same spectrum only spectrally shifted.

4. ACTIVE POLARIZATION CONTROL

In our first experiment light was sent through the input fiber aligned with one of the 1D grating coupler as indicated in Fig. 6. The light going through the system was coupled out through the 2D grating coupler into a fiber. A collimator focused the light into free space and a polarization beam splitter separated the light into

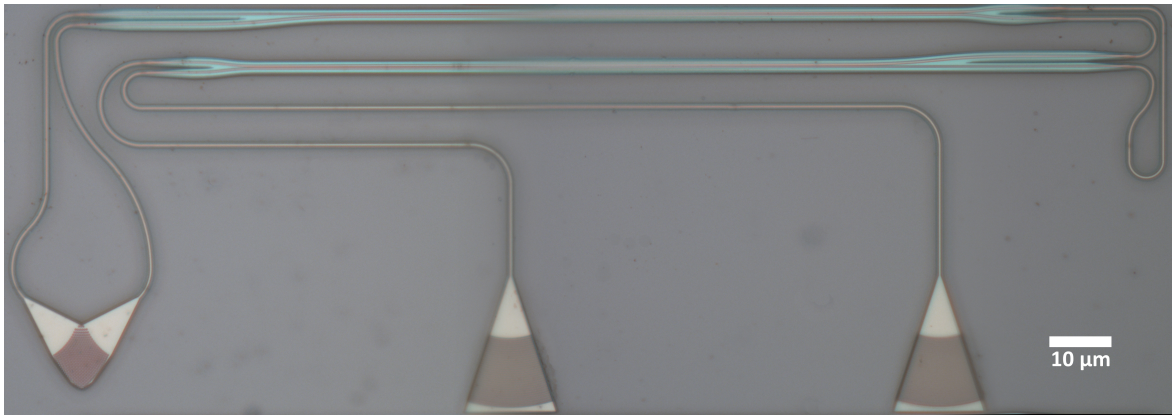

Figure 4. An optical micro graph of the fabricated system.

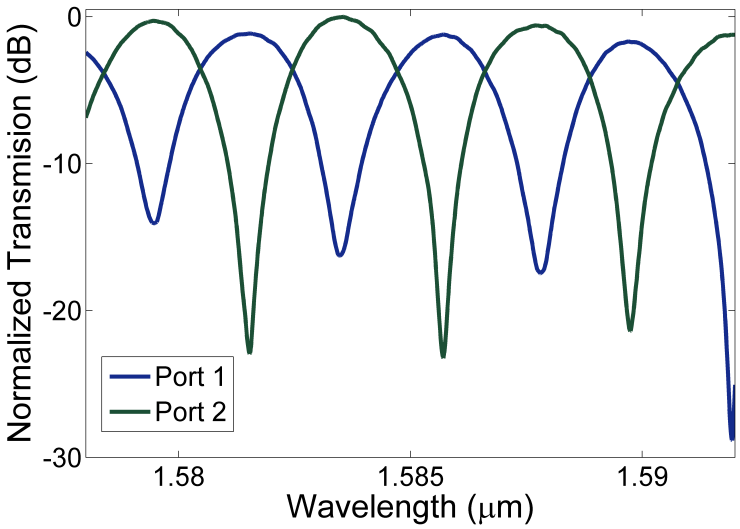

Figure 5. Normalized transmission spectrum of the device shown in Fig. 4. The light is injected into the 2D grating coupler and the transmission at the two 1D grating couplers (Port 1 & 2) is measured. Due to the offset in the MZI a beating pattern as function of wavelength is observed.

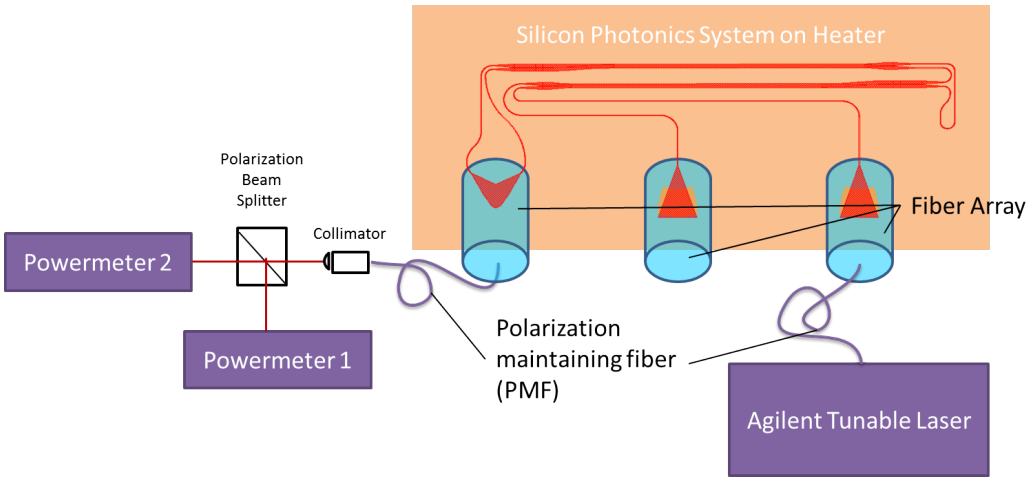

Figure 6. Schematic representation of the first proof of principle measurement. In this case the tuning of the polarization was demonstrated.

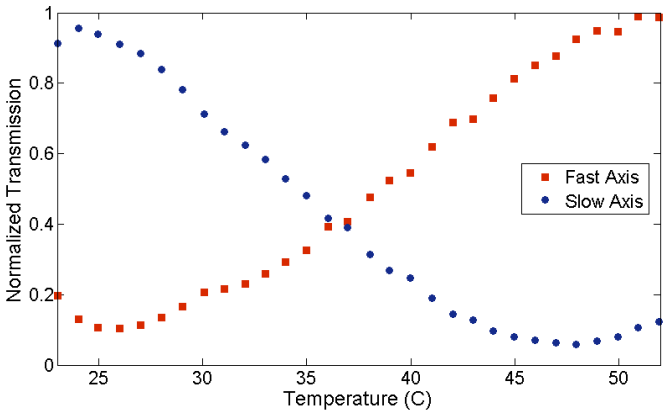

Figure 7. Normalized transmission of our system with light incident on one 1D grating coupler and coupled off through the 2D grating coupler. As the sample is heated light is switched between light polarized along the fast axis of the polarization maintaining fiber and light polarized along the slow axis.

its two orthogonal polarization components. The two components are when the light is either polarized along the fast axis or along the slow axis of the polarization maintaining fiber. The power in the two components as a function of sample temperature is plotted in Fig. 7. The power switches between the two polarizations as the temperature increases. This switching is the direct result of the change in phase shift in the unbalanced MZI, which then leads to a change in output power distribution. These results were obtained at a wavelength of 1.55 μm. Other wavelengths showed similar behavior with a temperature shift for maximum transmission of a specific polarization state.

5. POLARIZATION TRANSPARENCY

A schematic of the next experiment is shown in Fig. 8. Light from an Agilent tunable laser source is coupled to free-space and send through a polarizer, half-wave plate and lastly a quarter wave-plate. The wave-plates are used to get full control over the polarization state of light. The light is then focused back into a polarization maintaining fiber and coupled to the 2D grating coupler on the chip. The output of the polarization transparency circuit is monitored by coupling the light of the chip using two 1D grating coupler designed for the TE mode of a silicon waveguide.

We measured the insertion loss of the setup and fiber to coupler first. The 2D grating coupler had an insertion loss of 13 dB, the 1D grating coupler had a coupling loss of 8.3 dB, and the free space coupling setup a loss of

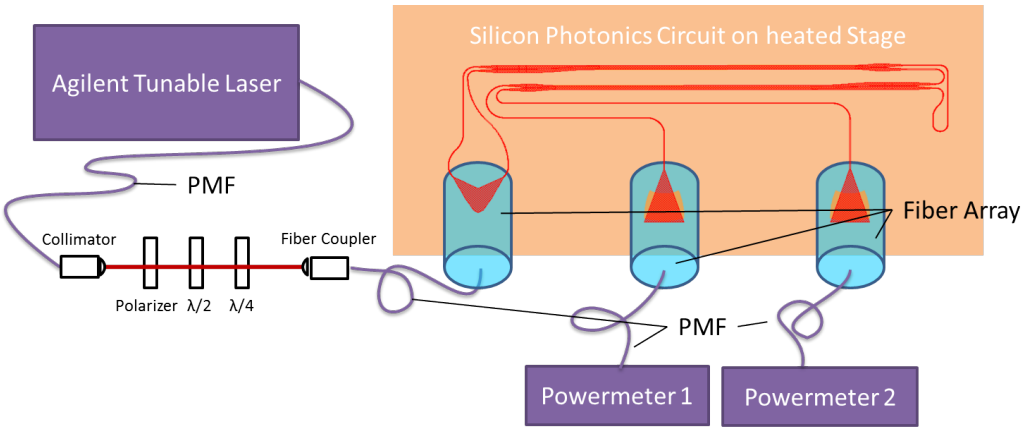

Figure 8. Schematic representation of the second proof of principle measurement. Successful coupling of different linear polarization to one output with high extinction was demonstrated.

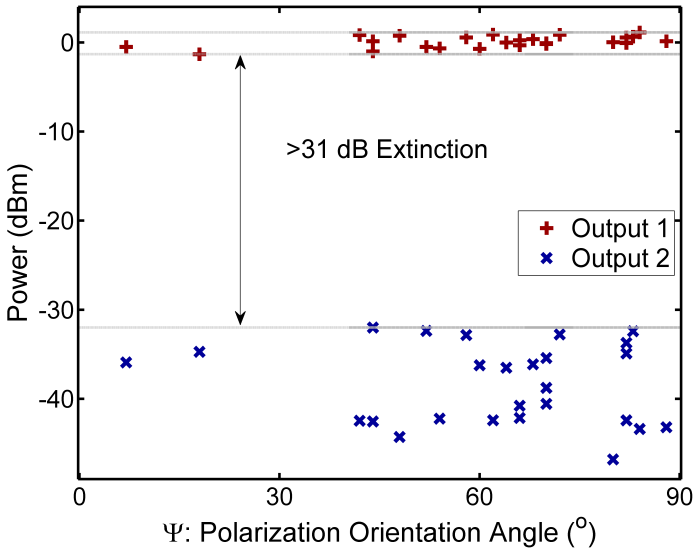

Figure 9. Normalized transmission of the proof of concept polarization transparency system as a function of input polarization angle (ψ). More then 25 polarization states where all coupled to one polarization in one waveguide.

9.2 dB. The loss of the grating couplers was higher then previous results[10,14] as the 2D grating coupler and 1D grating coupler were accidentally designed for different angles, thus light was coupled from the fiber to the grating coupler at a suboptimal angle for both gratings, as the fibers can not be aligned separately. We subtracted then the insertion losses of the components from our polarization coupling results.

Here, we demonstrate that a number of different polarization states can all be coupled to the same output waveguide. The system was tuned again by changing the stage temperature and thus tuning the phase difference in the MZI located between the couplers. This MZI controls the power distribution between the two output polarization states. Due to the heat capacity of the whole stage it can take a few minutes to reach a specific temperature. Thus to allow for fast data acquisition, we would set the stage temperature to T_1 and then tune the wave-plates to find the polarization state that couples optimally. We would record the angles of the two wave-plates and then change the stage temperature to T_2 and repeat the previous procedure. This process was faster then preselecting the polarization state and then finding the matching temperature. A schematic of the setup is shown in Fig. 8

The angle between the two polarization states, that means the power distribution between the fast and slow mode in the polarization maintaining fiber can be calculated using the Jones matrix approach. In this case the angle of interest is the orientation angle ψ. ψ is the angle between the major axis of the polarization ellipse with the fast axis of the polarization maintaining fiber. The polarization angle was calculated using the recorded angles of the wave-plates which is explained in e.g.[18]

The experimental results of coupling a variety of polarization states to the silicon photonics circuit are shown in Fig. 9. The power was always coupled to Output 1 for all polarization states which had an orientation angle ranging between only a few degrees all the way up to 90^o. Output 2 was suppressed with an extinction of more than 31 dB. Output 1 had an average insertion loss of 0.07 dB, this is after accounting for external factors as discussed previously, with a standard deviation of 0.62 dB. The upper and lower bound where 1.1 dB and -1.3 dB. Thus the maximum variation of the output 1 is only 2.4 dB. This variation can be explained by thermal drifts in alignment of the free space coupling setup as well as the fiber to chip setup.

6. CONCLUSION

In summary in this first proof of principle experiment we successfully coupled more than 20 polarization states to a silicon photonics circuit. The light was collected in the TE mode of a single waveguide with less than 2.4 dB

variation and a system loss of only 0.07 dB. Additionally we have shown that an arbitrary linear polarization state can be created using our system. Furthermore we have theoretically derived the system response of an improved photonic circuit with two integrated heaters which we are currently in the process of fabricating.

ACKNOWLEDGMENTS

We gratefully acknowledge the financial support from the Natural Sciences and Engineering Research Council [NSERC] of Canada, in particular the Silicon Electronic Photonic Integrated Circuits (Si-EPIC) CREATE Program. J.N.C thanks NSERC for his Vanier CGS graduate fellowship. We thank CMC Microsystems for providing funding for sample fabrication and providing access to facilities. We thank Han Yun for the GDS layout of the adiabatic coupler and assistance with making them compatible with our system, additionally we thank him and Jonas Flueckiger for assistance with the measurements. Sample fabrication was performed by Richard Bojko at the the University of Washington –Washington Nanofabrication Facility (UW WNF), which is a national user facility that is a part of the National Nanotechnology Infrastructure Network (NNIN).

REFERENCES

[1] Pavesi, L. and Lockwood, D., [*Silicon Photonics*], Springer (2004).

[2] Barwicz, T., Watts, M. R., Popovic, M. A., Rakich, P. T., Socci, L., Kartner, F. X., Ippen, E. P., and Smith, H. I., "Polarization-transparent microphotonic devices in the strong confinement limit," *Nature Photonics* **1**(1) (2006).

[3] Taillaert, D., Van Laere, F., Ayre, M., Bogaerts, W., Van Thourhout, D., Bienstman, P., and Baets, R., "Grating Couplers for Coupling between Optical Fibers and Nanophotonic Waveguides," *Japanese Journal of Applied Physics* **45**, 6071–6077 (Aug. 2006).

[4] Noda, J., Okamoto, K., and Sasaki, Y., "Polarization-maintaining fibers and their applications," *Lightwave Technology, Journal of* **4**, 1071–1089 (Aug 1986).

[5] Zou, J., Yu, Y., Yang, W., Wu, Z., Ye, M., Chen, G., Liu, L., Deng, S., and Zhang, X., "An SOI based polarization insensitive filter for all-optical clock recovery," *Optics Express* **22**, 6647 (Mar. 2014).

[6] Bogaerts, W., Taillaert, D., Dumon, P., Van Thourhout, D., Baets, R., and Pluk, E., "A polarization-diversity wavelength duplexer circuit in silicon-on-insulator photonic wires.," *Optics express* **15**, 1567–78 (Feb. 2007).

[7] Doerr, C. R., "Proposed architecture for MIMO optical demultiplexing using photonic integration," *IEEE Photonics Technology Letters* **23**, 1573–1575 (Nov. 2011).

[8] Sacher, W. D., Barwicz, T., Taylor, B. J. F., and Poon, J. K. S., "Polarization rotator-splitters in standard active silicon photonics platforms," *Optics Express* **22**, 3777 (Feb. 2014).

[9] Miller, D. A. B., "Self-configuring universal linear optical component [Invited]," *Photonics Research* **1**, 1 (June 2013).

[10] Mekis, A., Gloeckner, S., Masini, G., Narasimha, A., Pinguet, T., Sahni, S., and De Dobbelaere, P., "A grating-coupler-enabled CMOS photonics platform," *Selected Topics in Quantum Electronics, IEEE Journal of* **17**(3), 597–608 (2011).

[11] Van Laere, F., Bogaerts, W., Dumon, P., Roelkens, G., Van Thourhout, D., and Baets, R., "Focusing polarization diversity gratings for Silicon-on-Insulator integrated circuits," *2008 5th IEEE International Conference on Group IV Photonics* **1**, 203–205 (2008).

[12] Yariv, A. and Yeh, P., [*Photonics: Optical Electronics in Modern Communications*], Oxford University Press (2007).

[13] Helmholtz, H., [*Handbuch der physiologischen Optik*], Leopold Voss (1856).

[14] Yun Wang, Jonas Flueckiger, C. L. and Chrostowski, L., "Universal grating coupler design," *Proc. SPIE, Photonics North 2013* **8915**, 89150Y (06/2013 2013).

[15] Yun, H., Shi, W., Wang, Y., Chrostowski, L., and Jaeger, N. A. F., "2x2 adiabatic 3-db coupler on silicon-on-insulator rib waveguides," *Proc. SPIE, Photonics North 2013* **8915**, 89150V (June 2013).

[16] Chrostowski, L. and Hochberg, M., [*Silicon Photonics Design*], Cambridge University Press (2014).

[17] Lin, C., "Photonic device design flow : from mask layout to device measurement.", MASc, University of British Columbia (2012)
[18] Saleh, B. E. A. and Teich, M. C., [*Fundamentals of Photonics*], Wiley (2007).